THE JOURNAL OF PHYSICAL CHEMISTRY C

Article

pubs.acs.org/JPCC

Helium Atom Scattering from Graphene Grown on Rh(111)

K.D. Gibson and S. J. Sibener*

The James Franck Institute and Department of Chemistry, The University of Chicago, 929 East 57th Street, Chicago, Illinois 60637, United States

ABSTRACT: Graphene growth on transition-metal surfaces leads to an ordered superlattice that appears as a series of hills and valleys in scanning tunneling microscopy. On Rh(111), the graphene forms an incommensurate epitaxial overlayer; the crystallographic axes of the graphene are closely aligned with the Rh(111) surface lattice vectors, but the Rh and graphene lattice constants are significantly different. Thus, the C atoms sit over different positions of the Rh(111) lattice and their height above the Rh(111) surface varies, but the different binding sites also affect the local electronic structure. Scanning tunneling microscopy is affected by both of these factors. He scattering is more a measure of the geometrical corrugation, the variation of the height of the graphene sheet relative to the Rh(111) surface. We compare the results of He diffraction measurements with those of previous scanning tunneling microscopy measurements to assess the relative geometric and electronic corrugations.

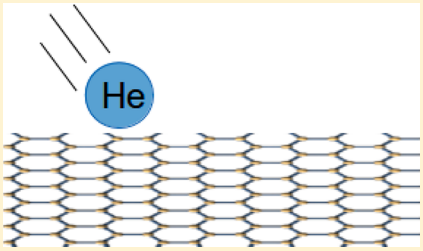

INTRODUCTION

There is intense interest in graphene, a single layer of sp^2 bonded C, analogous to the top (0001) layer of graphite, because of the remarkable chemical, physical, and electronic properties of this two-dimensional material. We concentrate on the growth of graphene on a transition metal.[1,2] Specifically, we examined the structure of graphene on the (111) face of Rh (a face-centered cubic crystal), using ethylene as the precursor.

Our present study was motivated by a paper by Borca et al.[3] in which they examined epitaxial graphene on Ru(0001) using a combination of scanning tunneling spectroscopy (STM) and He atom scattering (HAS). Relative to other transition metals, graphene is strongly bonded with Ru(0001)[1,4,5] and forms an incommensurate epitaxial overlayer. There is a large scale Moiré pattern observed by STM (lattice constant, ~3 nm), and the Ru(0001) and graphene crystallographic axes closely align.[3,6] The Moiré pattern is due to the different lattice constants for graphene (0.246 nm) and Ru(0001) (0.27 nm). The lack of registry results in C atoms being adsorbed over many different locations on the Ru(0001) surface, with a repeat distance of ~12 graphene hexagons to 11 Ru atoms, leading to a long-range ripple in the graphene overlayer perpendicular to the surface. Borca et al. found that the STM gave a perpendicular corrugation of greater than 0.1 nm, whereas the HAS results gave a corrugation of ~0.015 nm. They explain this discrepancy by suggesting that the STM results are electronic in nature and the geometrical corrugation, the actual positions of the individual C atoms, is determined by the HAS data. However, density functional theory (DFT) calculations,[4,7] low-energy electron diffraction (LEED) results,[8] and surface X-ray diffraction experiments[9,10] all indicate that the geometrical corrugation is much larger than 0.015 nm.

The corrugation measured by HAS can be different than that measured by STM. Briefly, for low translational energy He atoms, the interaction is with the surface electron density in the vicinity of the atom−surface collision.[11] This should follow the ripple in the graphene perpendicular to the metal surface caused by the C atom−transition-metal surface plane distance changing dependent upon the position of the C atoms within the metal surface unit cell, i.e., the geometrical corrugation. STM involves measuring the sample−tip tunneling current, dependent upon the overlap between the tip and surface wave functions, and so the measured corrugation will change with parameters such as the tip−surface bias potential.[12] For example, Voloshina et al.[13] saw the corrugation for graphene on Rh(111) change from 0.05 to 0.15 nm depending upon the imaging conditions.

The C is often deposited by exposing the clean, hot (~900−1100 K) Rh(111) surface to ethylene, though other molecules such as acetylene[14] and 3-pentanone[15] have also been used. The surface temperature and exact dosing procedure may have an effect on the quality of the resulting overlayer.[16] The surface must be hot enough for the precursor to decompose but not so hot that the C can dissolve into the bulk.[17] With the proper surface temperature, only a single layer of C, the graphene sheet, is adsorbed because the decomposition of the ethylene occurs only on the metal surface, not on top of the graphene.[18] Among the transition metals studied, graphene has a relatively strong interaction with Rh.[1,5,19] As shown by STM and LEED, the graphene layer forms an incommensurate epitaxial overlayer on Rh(111); it is aligned with the Rh(111) crystallographic axes with a ratio of ~12 C hexagons/11 Rh (graphene lattice constant, 0.246 nm; Rh(111) lattice constant, 0.269 nm).[5,13−15,19,20] As with Ru(0001), C atoms have a spacing different than that of the underlying Rh; over the 11 Rh repeat

Special Issue: John C. Hemminger Festschrift

Received: April 24, 2014
Revised: May 13, 2014
Published: May 30, 2014

   dx.doi.org/10.1021/jp504024t | J. Phys. Chem. C 2014, 118, 29077−29083

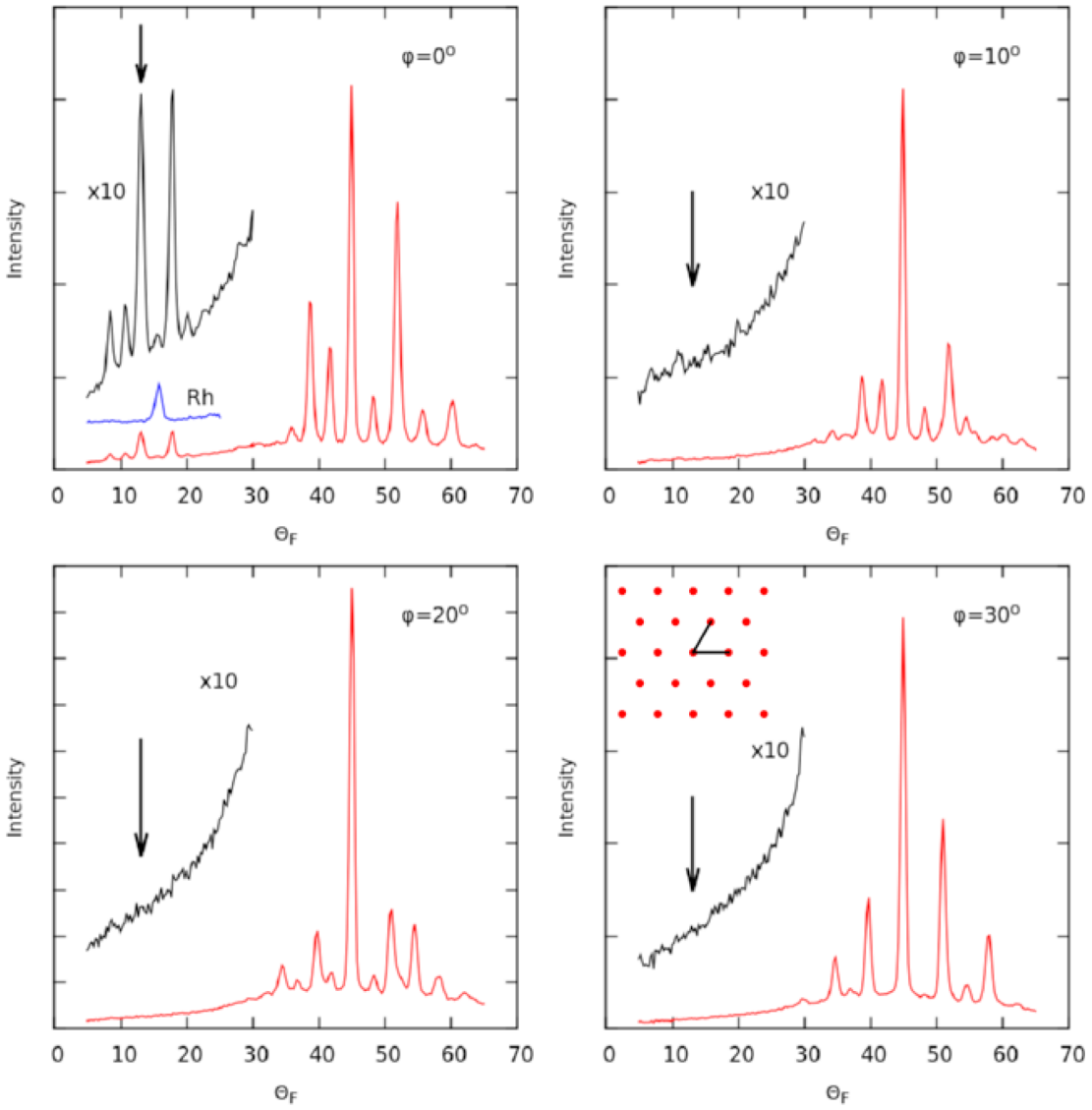

Figure 1. He diffraction spectra at $\theta_I = 45°$, $T_S = 200$ K, and $\langle E_I \rangle = 19.7$ meV. $\phi = 0°$ is the $\langle 11\bar{2} \rangle$ direction, and $\phi = 30°$ is the $\langle 10\bar{1} \rangle$ direction for the Rh(111) substrate. Arrows indicate the position where the (11) diffraction peak due to the graphene would occur. The inset for $\phi = 30°$ schematically shows the hexagonal placement of the atoms on the Rh(111) surface, along with the two unit vectors. Also shown is the clean Rh(111) first-order diffraction peak for $\phi = 0°$.

distance, they lie in different positions within this larger unit cell: near atop, hollows, and bridge sites of the Rh(111).[13,19,20] The result is a ripple in the graphene overlayer perpendicular to the surface plane of the Rh(111), resulting in a Moiré pattern having a rhombus-shaped unit cell with a lattice constant of ~2.9 nm and much internal structure.

We will describe our experiments using HAS to examine the growth and structure of the graphene on Rh(111). In particular, we will examine the relative corrugation amplitudes given by HAS and STM measurements.

EXPERIMENTAL SECTION

The experimental apparatus consisted of an ultrahigh vacuum (UHV) chamber with a base pressure of $\sim 2 \times 10^{-10}$ Torr. As many as three separate molecular beams, produced in a source chamber with multiple stages of differential pumping, could converge on the target crystal simultaneously. The detector consisted of an electron bombardment ionizer and a double differentially pumped quadrupole mass spectrometer, which could be moved in an arc around the position of the target, with a full width at half-maximum (fwhm) angular acceptance of ~1°. The plane of the arc defined by the detector motion is then the scattering plane within which the He was detected after colliding with the target. The target was welded to a three-axes mount that allowed for the independent adjustment of the incident angle of the molecular beam (θ_I, measured relative to the surface normal), the in-plane rotation of the target crystal (ϕ, the azimuth), and the tilt of the surface relative to the scattering plane. For the experiments described, the tilt was adjusted so that the surface plane was perpendicular to the scattering plane. The angle between the detector and the normal to the target surface is θ_F. The target was resistively heated and cryogenically cooled. Surface temperature (T_S) was measured with a chromel−alumel thermocouple welded to the target crystal.

The target was a Rh single crystal, cut and polished to within better than 1° of the (111) face as determined by Laue X-ray backscattering. Cleaning was done by cycles of Ar^+ bombard-

dx.doi.org/10.1021/jp504024t | J. Phys. Chem. C 2014, 118, 29077−29083

ment and O_2 exposure, both at 900 K. Annealing was done at ~1250 K. Initial cleanliness was checked with Auger electron spectroscopy (AES). After each cycle of cleaning and annealing, the He specular refection was checked. After many cycles, the intensity of the reflection reached a constant value, and this value could be used to assess surface cleanliness. Normal cleaning during the course of the experiments required only a short O_2 exposure and 3 min anneal. Many graphene layers were grown during the course of these experiments, and it was found that the most sensitive method for determining whether all of the C was removed before a new layer was deposited was to use the He specular reflectivity of the Rh(111) surface. A small amount of C led to a large attenuation of the signal, as explained by Poelsema and Comsa.[21]

Dosing was done with a neat beam of ethylene (Matheson, Research grade, > 99.99% purity) or acetylene (Matheson, Purified, 99.6% purity), expanded through a 200 μm nozzle with a 200 Torr stagnation pressure and θ_I = 45°. As determined by the pressure rise in the UHV chamber, pumping speed, and diameter of the beam, we estimate that the flux was ~10^{14} cm^{-2} s^{-1}.

The He scattering was done with two different translational energies, accomplished by expanding high-pressure He (200 to 400 psig) through a 10 μm pinhole. Beam velocities were determined by a time-of-flight (TOF) technique. The target could be lowered out of the beam path, and the detector rotated so the beam impinged directly on the ionizer. A rotating wheel with small slots mechanically chopped the beam, and by measuring the He signal in a series of small time bins of equal length and knowing the distances, it was possible to determine the energy and energy spread of the beams. When cooled with liquid N_2, a typical beam had an average translational energy ($\langle E_I \rangle$) of 19.7 meV with a $\Delta E/\langle E_I \rangle$ = 0.04 fwhm. With the nozzle at ambient temperature, a typical beam had an $\langle E_I \rangle$ = 65.3 meV with a $\Delta E/\langle E_I \rangle$ = 0.12 fwhm.

For the scattering measurements, the rotating chopper had large slots and time-integrated data were taken while the slot allowed He through, with a detector background correction measured when the chopper blocked the beam. It is important to note that the detector looked at scattering from an area with dimensions on the order of 1 mm. In contrast to STM measurements, which examine areas with dimensions of a few nanometers in detail, HAS gives information averaged over quite macroscopic regions.

RESULTS AND DISCUSSION

Figure 1 shows example He diffraction spectra, taken with $\langle E_I \rangle$ = 19.7 meV and θ_I = 45°, along several azimuths (ϕ = 0° is the $\langle 11\bar{2} \rangle$ direction and ϕ = 30° is the $\langle 10\bar{1} \rangle$ direction for the Rh(111) substrate). The surface was grown using ethylene, dosing for 5 min at 300 K, heating to 1070 at 100 K min^{-1}, dosing for a further 10 min, and then immediately cooling to 200 K. The large features around the specular are due to the Moiré pattern and give a lattice constant of 2.95 ± 0.05 nm, in agreement with STM results of 2.93 ± 0.13[15] and 2.90 ± 0.05[20] nm. At ϕ = 0°, the arrow indicates the position of the first-order diffraction peak expected for the graphene sheet. Around this feature, there are peaks due to the superlattice. At the other azimuths shown, there is no indication of this feature. We measured diffraction at azimuths near 0°, and the diffraction feature disappears within ±2° of the ⟨11⟩ direction. This is strong evidence that much of the graphene is very closely aligned with the Rh(111) surface, but does not rule out the possibility of some domains aligned at a few other azimuths, as is the case for graphene on Ir(111).[18,22] At T_S = 200 K and with the base pressure of 2 × 10^{-10} Torr, the graphene was stable for several hours, as determined by the positions and relative intensities of the diffraction features.

The angular widths of the elastic features are dependent on the size of the ordered graphene domains.[23] Within our measurement error, the widths are the same as the instrumental transfer width,[24] meaning that the ordered domains have average dimensions as large or larger than ~13 nm. These narrow diffraction features are superimposed upon a broad lobular background. If we make time-resolved measurements at angles between the elastic features, we find both the expected inelastic scattering and a rather large incoherent elastic peak. The latter is usually the result of scattering from defects in the surface that modify the local surface normal, but we do not know the nature of the defects.

We experimented with different surface temperatures and dosing procedures to determine how to reproducibly grow the best graphene overlayers as determined by He diffraction. Again, it is important to note that HAS measures the structure over macroscopic distances. The quality of the graphene overlayer was judged by the lattice constant, widths of the diffraction features, and intensity of the diffraction peaks relative to the specular diffraction peak. The specular reflection from clean Rh was ~100× the intensity from a good graphene overlayer. Thus, even small areas of uncovered Rh can lead to large specular signals, indicating whether the Rh is completely covered. It was suggested by Dong et al.[16] that the best overlayers were produced by first dosing at temperatures below the graphene formation temperature and then heating to the final temperature and redosing. Our normal procedure was to dose the clean Rh(111) for 5 min at T_S = 300 K. The surface was then heated to the final temperature at 100 K min^{-1} and exposed for an additional 10 min. However, we found that the most important factors were initial crystal cleanliness and the final surface temperature. The best temperature was in the vicinity of 1070 K, and the diffraction data were nearly the same even when the clean surface was dosed only at the elevated T_S. This is close to the temperature at which Dong et al.[16] found that only graphene was formed (no carbide) and below which there is appreciable dissolution of the C into the Rh. AES indicated that even a 30 min dose at 1070 K did not lead to an increase in the C signal, indicating that a limit had been reached, presumably a monolayer. When dosing at 1170 K, there was considerably more C after a 10 min dose than when dosing at 1070 K. The nonspecular diffraction features were very small and broad and did not occur at angles consistent with the expected Moiré pattern. Likewise, dosing at 1000 K lead to a diffraction pattern indicative of a much more poorly ordered graphene overlayer.

To determine the corrugation, it is necessary to do some form of scattering calculation. Good reviews of using He scattering for the structural determination of surfaces were authored by Reider et al.[24,25] We opted for the simplest approach, the eikonal approximation,[24−27] using a corrugated hard wall approximation that ignores the attractive part of the He−surface interaction potential.

$$A_{\mathbf{G}} \propto \int_{uc} \exp(-i[\mathbf{G}\cdot\mathbf{R} + (k_{\mathbf{G}}(z) - k_I(z))\zeta(\mathbf{R})])\, d\mathbf{R} \quad (1)$$

where $\mathbf{R}$ is the position and $\mathbf{G}$ is a reciprocal lattice vector. $k_{\mathbf{G}}(z) = k_I \cos(\theta_F)$ and $k_I(z) = -k_I \cos(\theta_I)$; k_I is the magnitude

dx.doi.org/10.1021/jp504024t | J. Phys. Chem. C 2014, 118, 29077−29083

of the incident wavevector, and the integration is over the unit cell. $\zeta(\mathbf{R})$ is the surface corrugation function. The scattering probability for any diffraction feature is then given by

$$P_{\mathbf{G}} = [\cos(\theta_F)/\cos(\theta_I)]|A_{\mathbf{G}}|^2 \quad (2)$$

The corrugated hard wall approximation is that $V(z) = 0$ for $z > \zeta(\mathbf{R})$ and $V(z) = \infty$ for $z \leq \zeta(\mathbf{R})$. The combination of eikonal and corrugated hard wall approximations is valid only for θ_I near normal and with $\langle E_I \rangle$ much greater than D, the depth of the actual He−surface potential. Boato et al.[28] found the laterally averaged D for the (0001) surface of graphite to be ∼15 meV, so we used a He beam with $\langle E_I \rangle$ = 65.3 meV for the diffraction measurements to be compared with the calculations. Another requirement is that the lattice constant be much greater than the corrugation. This is satisfied in our case because the superlattice structure has a lattice constant of ∼3 nm, whereas the expected corrugation is on the order of 0.1 nm.

The next step is to determine a model for $\zeta(\mathbf{R})$. A simple approach is to treat the surface corrugation as the sum of two different lattices; the graphene sheet lying over the larger lattice that produces the Moiré pattern, with their surface crystallographic axes aligned. We modeled the graphene sheet after the top layer of graphite.[28] It is aligned with the crystallographic axes of the Rh(111), and the corrugation has a cosine modulation with a repeat distance of 0.246 nm and a prefactor of 0.01 nm, which gives a peak-to-peak modulation of 0.02 nm, the value for the (0001) surface of graphite.[28] An approximation of the larger unit cell can be obtained from the STM results.[20] The unit cell is a rhombus with sides of 2.95 nm. Two of the sides, which have a common origin and an included angle of 60°, are formed from the ⟨10⟩ and ⟨01⟩ surface lattice vectors. The long diagonal is the ⟨11⟩ direction. At each corner are identical large features, and along the ⟨11⟩ direction are two symmetrical protrusions, as seen in the STM.[20]

Figure 2 shows some diffraction scans for $\langle E_I \rangle$ = 65.3 meV. They show quite large features near specular which are due to the Moiré pattern. The arrows indicate the positions of the elastic features due to the graphene periodicity. The diffraction features could be fit with Gaussians, and the area used to determine the scattering probability. We neglected the Debye−Waller correction, which takes into account the inelastic scattering.[24,25] For comparison, the main consideration is the dependence of the Debye−Waller factor on final angle. However, we felt that this did not have a significant effect on qualitative results for the small range of angles used for the comparison between experiment and calculation. The experimental results are shown in Figure 3, along with the results calculated using the eikonal approximation. These calculations were done in a least-squares sense, with features of the large Moiré rhombus being the variable parameters. Specifically, these were the large features at the four corners; their positions were fixed and they were represented by a two-dimensional Gaussian having rotational symmetry around the surface normal, but the height and width were variable. The two smaller features along the ⟨11⟩ direction, which were constrained to be identical and symmetrically distributed about the center of the unit cell, were also represented by two-dimensional Gaussians with rotational symmetry around the surface normal, but with the height, width, and position along the ⟨11⟩ direction variable. Finally, the last variable was a multiplier to match the calculations to the experiments.

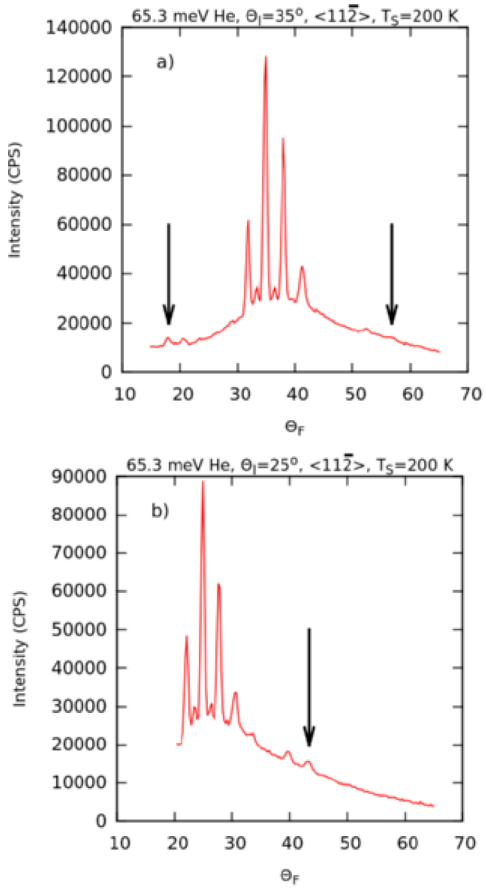

Figure 2. He diffraction spectra at θ_I of 35° (panel a) and 25° (panel b); T_S = 200 K, $\langle E_I \rangle$ = 65.3 meV, and ϕ = 0°. Arrows indicate the position where the (11) diffraction peak due to the graphene would occur.

The Moiré corrugation function is shown in Figure 4, without the superimposed graphene corrugation. As is evident from Figure 3, this is a rather crude estimate of the true corrugation, but qualitatively gives a reasonable agreement with the experiment. The important result is that the He scattering results give a significant corrugation, ∼0.09 nm, a value which is in agreement with the corrugation measured by STM experiments. This is in significant contrast to the results for graphene on Ru(0001) measured by Borca et al.[3] (see their Figure 4). Though the He beam energies are different, it is telling that the intensities of the diffraction peaks are small relative to the specular, in contrast to the ratios that we see for graphene on Rh(111). As can be seen by examining eq 1, the intensities of the nonspecular features relative to the specular increase as the corrugation increases. For comparison, we did an eikonal calculation for a corrugation of 0.015 nm, the value that Borca et al.[3] determined. The results are shown in Figure 5a, and all of the nonspecular diffraction features are very small. Just the appearance of our diffraction spectra relative to those from Borca et al.[3] would suggest that the graphene on Rh(111) is more corrugated than suggested by the He diffraction results for graphene on Ru(0001).

As mentioned, we were able to grow the large graphene domains over only a very limited range of surface temperatures. The surface temperature we used, 1070 K, is very close to that at which Dong et al.[16] found that only graphene is formed and there is no dissolution into the bulk. Figure 5b shows a

dx.doi.org/10.1021/jp504024t | J. Phys. Chem. C 2014, 118, 29077−29083

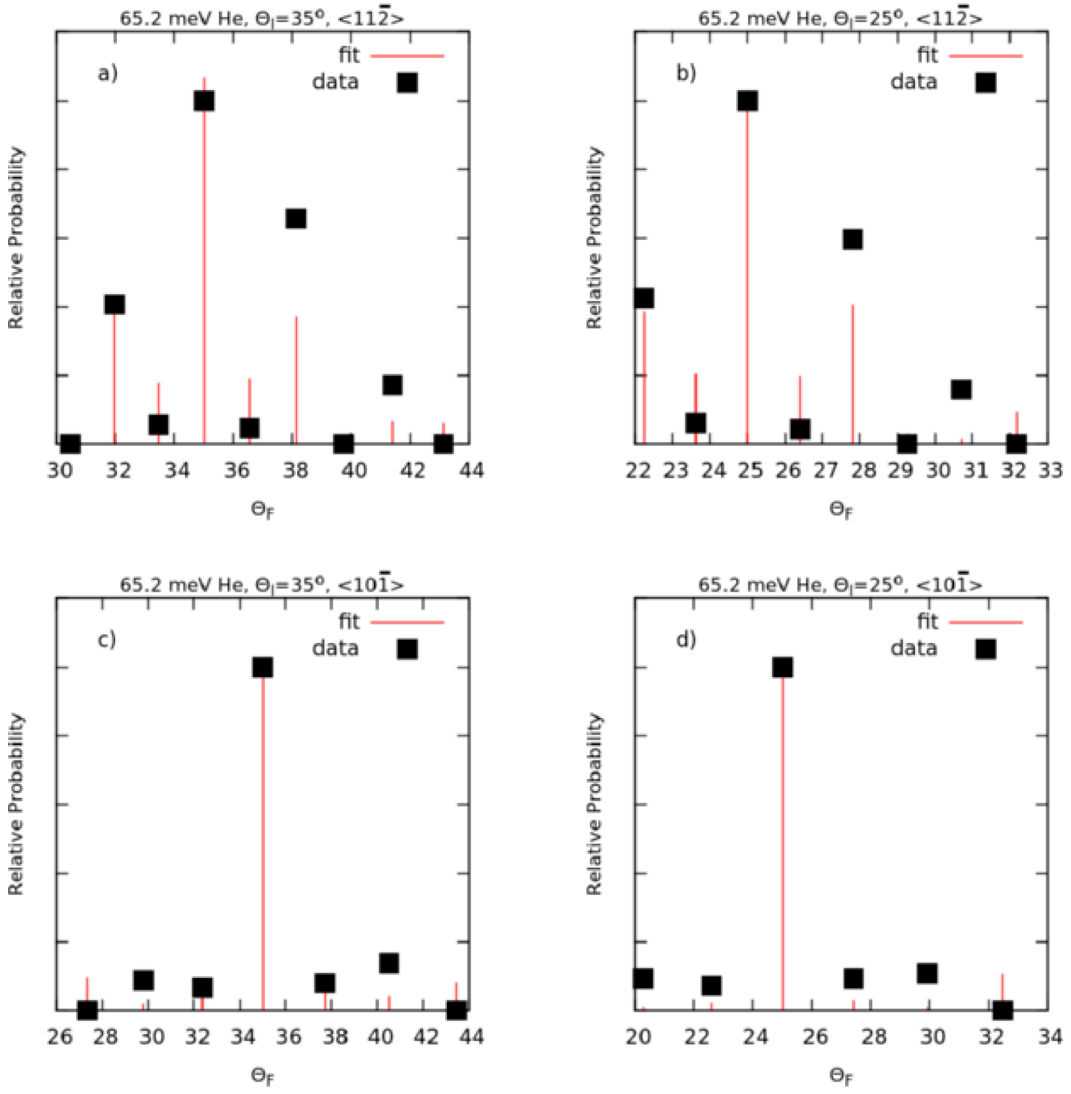

Figure 3. Comparison of experimental results and the eikonal calculations. He diffraction spectra taken at T_S = 200 K, $\langle E_I \rangle$ = 65.3 meV, and with ϕ = 0° and 30°.

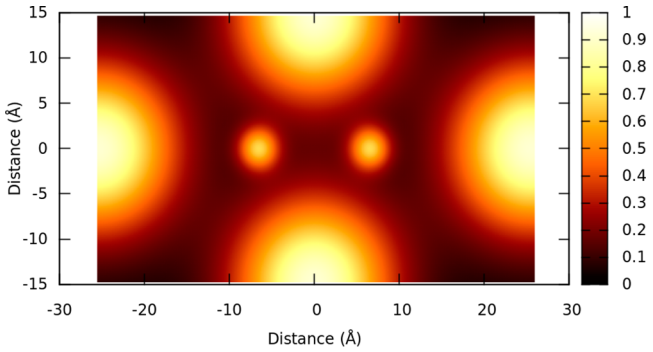

Figure 4. Contour plot of the superlattice corrugation derived from the eikonal calculations (see text). For clarity, the ripple due to the graphene has been omitted.

diffraction spectrum taken after exposing the clean Rh(111) surface to C_2H_4 at T_S = 1000 K. Under this condition, both carbide and graphene can form.[16] Compared with the spectra in Figure 1, there are fewer diffraction features, and the specular is quite large by comparison. Qualitatively, this is more like the diffraction results of Borca et al.[3] Though our substrate is Rh rather than Ru, this does suggest that one possibility is that their surface conditions were not exactly right for growing the large graphene domains. Once again, it is important to note that He scattering is sensitive to the order over macroscopic areas.

■ CONCLUSIONS

We presented HAS results for graphene grown on Rh(111). We found a method for growing a reproducible overlayer, as determined by He scattering, dependent on surface temperature and surface cleanliness. The HAS results indicated that the crystallographic axes of the Rh(111) substrate and the graphene were very closely aligned, and the resulting incommensurate epitaxial overlayer gave a rhombus-shaped superlattice cell with a lattice constant of 2.95 nm. A comparison of the experimental data and an eikonal scattering calculation gave a corrugation of ∼0.09 nm. The structure derived from the HAS results is only approximate; it is not meant to be a precise replica of the structure, but the HAS and STM give similar results for the corrugation. However, at least on Ru(0001), it was found that the corrugation determined by HAS (∼0.015 nm) and that determined by STM (∼0.1 nm)

dx.doi.org/10.1021/jp504024t | J. Phys. Chem. C 2014, 118, 29077−29083

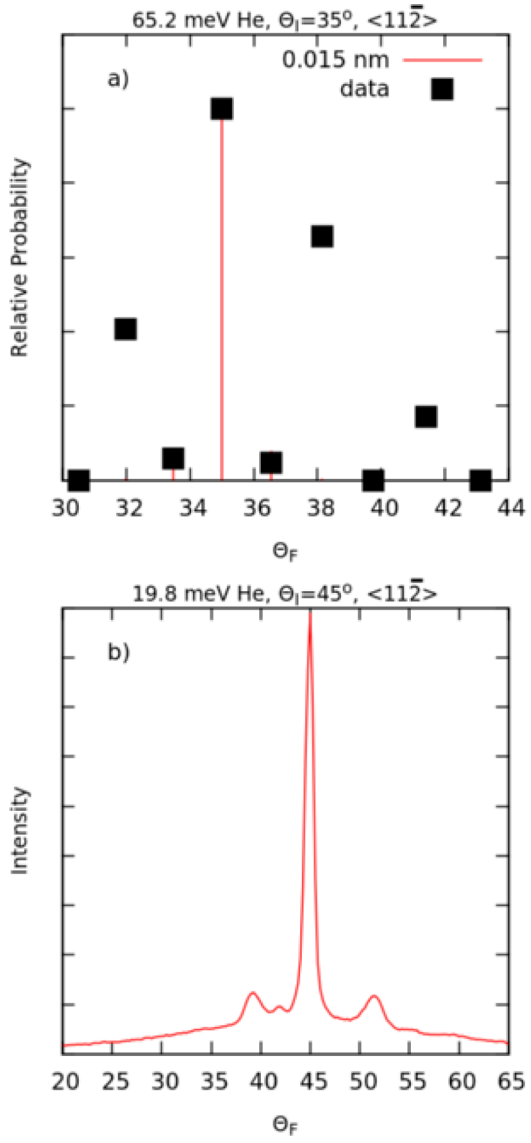

Figure 5. Panel a shows a comparison of the experimental results and the eikonal calculation using a corrugation of 0.015 nm. For the second- and higher-order diffraction peaks, the calculated intensities are too small to show up on the plot. Panel b shows the diffraction spectra for a graphene surface grown with different experimental conditions (see text).

were considerably different.[3] This suggests that the geometric corrugation is rather small and the corrugation seen in STM experiments is due to electronic effects. Our results for graphene on Rh(111) demonstrate that the geometric corrugation is actually a large part of the corrugation seen by the STM.

AUTHOR INFORMATION

Corresponding Author

*E-mail: s-sibener@uchicago.edu. Tel.: 773-702-7193.

Notes

The authors declare no competing financial interest.

ACKNOWLEDGMENTS

This work was supported by the Office of Basic Energy Sciences, U.S. Department of Energy, Grant DE-SC0002583, with further support for this project coming from the Air Force Office of Scientific Research Grant FA9550-10-1-0219. Infrastructure support from the NSF-Materials Research Science and Engineering Center at The University of Chicago is also gratefully acknowledged.

REFERENCES

(1) Batzill, M. The Surface Science of Graphene: Metal Interfaces, CVD Synthesis, Nanoribbons, Chemical Modifications, and Defects. *Surf. Sci. Rep.* **2012**, *67*, 83−115.
(2) Wintterlin, J.; Bocquet, M.-L. Graphene on Metal Surfaces. *Surf. Sci.* **2009**, *603*, 1841−1852.
(3) Borca, B.; Barja, S.; Garnica, M.; Minniti, M.; Politano, A.; Rodriguez-Garcia, J. M.; Hinarejos, J. J.; Farias, D.; Vazquez de Parga, A. L.; Miranda, R. Electronic and Geometric Corrugation of Periodically Rippled, Self-Nanostructured Graphene Epitaxially Grown on Ru(0001). *New J. Phys.* **2010**, *12*, 093018/1−093018/15.
(4) Wang, B.; Bocquet, M.-L.; Marchini, S.; Günther, S.; Wintterlin, J. Chemical Origin of a Graphene Moiré Overlayer on Ru(0001). *Phys. Chem. Chem. Phys.* **2008**, *10*, 3530−3534.
(5) Preobrajenski, A. B.; Ng, M. L.; Vinogradov, A. S.; Mårtensson, N. Controlling Graphene Corrugation on Lattice-Mismatched Substrates. *Phys. Rev. B* **2008**, *78*, 073401/1−4.
(6) Marchini, S.; Guenther, S.; Wintterlin, J. Scanning Tunneling Microscopy of Graphene on Ru(0001). *Phys. Rev. B* **2007**, *76*, 075429/1−075429/9.
(7) Jiang, D.; Du, M.-H.; Dai, S. First Principles Study of the graphene/Ru(0001) Interface. *J. Chem. Phys.* **2009**, *130*, 074705/1−074705/5.
(8) Moritz, W.; Wang, B.; Bocquet, M.-L.; Brugger, T.; Greber, T.; Wintterlin, J.; Günther, S. Structure Determination of the Coincidence Phase of Graphene on Ru(0001). *Phys. Rev. Lett.* **2010**, *104*, 136102/1−136102/4.
(9) Martoccia, D.; Willmott, P. R.; Brugger, T.; Björck, M.; Günther, S.; Schlepütz, C. M.; Cervellino, A.; Pauli, S. A.; Patterson, B. D.; Marchini, S.; et al. Graphene on Ru(0001): A 25 × 25 Supercell. *Phys. Rev. Lett.* **2008**, *101*, 126102/1−126102/4.
(10) Martoccia, D.; Björck, M.; Schlepütz, C. M.; Brugger, T.; Pauli, S. A.; Patterson, B. D.; Greber, T.; Willmott, P. R. Graphene on Ru(0001): A Corrugated and Chiral Structure. *New J. Phys.* **2010**, *12*, 043028/1−043028/12.
(11) Esbjerg, N.; Norskov, J. Dependence of the He-Scattering Potential at Surfaces on the Surface-Electron-Density Profile. *Phys. Rev. Lett.* **1980**, *45*, 807−810.
(12) Bai, C. *Scanning Tunneling Microscopy and Its Applications*, 2nd ed.; Springer Series in Surface Sciences; Springer: New York, 2000.
(13) Voloshina, E. N.; Dedkov, Y. S.; Torbruegge, S.; Thissen, A.; Fonin, M. Graphene on Rh(111): Scanning Tunneling and Atomic Force Microscopies Studies. *Appl. Phys. Lett.* **2012**, *100*, 241606/1−241606/4.
(14) Castner, D.; Sexton, B.; Somorjai, G. LEED and Thermal Desorption Studies of Small Molecules (H_2, O_2, CO, CO_2, NO, C_2H_4, C_2H_2 and C) Chemisorbed on the Rhodium (111) and (100) Surfaces. *Surf. Sci.* **1978**, *71*, 519−540.
(15) Roth, S.; Osterwalder, J.; Greber, T. Synthesis of Epitaxial Graphene on Rhodium from 3-Pentanone. *Surf. Sci.* **2011**, *605*, L17−L19.
(16) Dong, G. C.; van Baarle, D. W.; Rost, M. J.; Frenken, J. W. M. Graphene Formation on Metal Surfaces Investigated by in-Situ Scanning Tunneling Microscopy. *New J. Phys.* **2012**, *14*, 053033/1−053033/15.
(17) Rut'kov, E.; Kuz'michev, A.; Gall', N. Carbon Interaction with Rhodium Surface: Adsorption, Dissolution, Segregation, Growth of Graphene Layers. *Phys. Solid State* **2011**, *53*, 1092−1098.
(18) Loginova, E.; Bartelt, N. C.; Feibelman, P. J.; McCarty, K. F. Factors Influencing Graphene Growth on Metal Surfaces. *New J. Phys.* **2009**, *11*, 063046/1−063046/20.

(19) Wang, B.; Caffio, M.; Bromley, C.; Früchtl, H.; Schaub, R. Coupling Epitaxy, Chemical Bonding, and Work Function at the Local Scale in Transition Metal-Supported Graphene. *ACS Nano* **2010**, *4*, 5773−5782.
(20) Sicot, M.; Leicht, P.; Zusan, A.; Bouvron, S.; Zander, O.; Weser, M.; Dedkov, Y. S.; Horn, K.; Fonin, M. Size-Selected Epitaxial Nanoislands Underneath Graphene Moiré on Rh(111). *ACS Nano* **2012**, *6*, 151−158.
(21) Poelsema, B.; Comsa, G. *Scattering of Thermal Energy Atoms from Disordered Surfaces*; Springer Tracts in Modern Physics; Springer-Verlag: New York, 1989.
(22) Loginova, E.; Nie, S.; Thuermer, K.; Bartelt, N. C.; McCarty, K. F. Defects of Graphene on Ir(111): Rotational Domains and Ridges. *Phys. Rev. B* **2009**, *80*, 085430/1−085430/8.
(23) Gibson, K. D.; Cerjan, C.; Light, J. C.; Sibener, S. J. Elastic Helium Scattering Studies of Ordered Overlayers of Ar, Kr, and Xe Physisorbed on Ag(111). *J. Chem. Phys.* **1988**, *88*, 7911.
(24) Farias, D.; Rieder, K.-H. Atomic Beam Diffraction from Solid Surfaces. *Rep. Prog. Phys.* **1998**, *61*, 1575−1664.
(25) Engel, T.; Rieder, K. H. Structural Studies of Surfaces with Atomic and Molecular Beam Diffraction. In *Structural Studies of Surfaces*; Springer Tracts in Modern Physics; Springer-Verlag: New York, 1982; Vol. *91*.
(26) Garibaldi, U.; Levi, A. C.; Spadacini, R.; Tommei, G. E. Quantum Theory of Atom-Surface Scattering: Diffraction and Rainbow. *Surf. Sci.* **1975**, *48*, 649−675.
(27) Shuttleworth, I. G. Analysis of the (3 × 3)-H/Cu(111) System Using Eikonal-Level Helium Atom Scattering Simulations. *Surf. Rev. Lett.* **2007**, *14*, 1089−1093.
(28) Boato, G.; Cantini, P.; Tatarek, R. Study of Gas-Graphite Potential by Means of Helium Atom Diffraction. *Phys. Rev. Lett.* **1978**, *40*, 887−889.